Non-branching Solutions for the Design of Planar Four-bar Linkages Using Task Velocity Specifications

Nina P. Robson, Texas A&M University; J. Michael McCarthy, University of California, Irvine

Abstract

This study looked at the use of three positions and two velocities to define algebraic design equations for the synthesis of planar two-bar linkages, which were solved to obtain multiple solutions. To ensure that the four-bar linkage constructed from two of the solutions moves smoothly through the given task, Filemon's construction and Waldron's circle diagrams were used. The main contribution of this study was that both methods were found to have direct application in the planar four-bar linkage synthesis theory with task positions and velocity specifications. The authors showed that the task positions provide the geometric features of the position synthesis, such as the pole triangle and Waldron's three-circle diagram, while the velocities can be used to reshape the coupler movement for non-branching solutions.

The examples in the end show how to obtain fully operational four-bar mechanisms using a combination of the Waldron and Filemon constructions. It is important to realize that the techniques described here are very useful for avoiding branching in planar four-bar linkages and can become a powerful tool for the future design of novel closed-loop mechanical systems.

Introduction

In this study, the authors considered the synthesis of planar RR chains to guide a floating link through five multiply separated positions (see Figure 1). The kinematic specification is three task positions with two specified velocities, denoted PP-P-PP [1], [2]. The goal in this study was to assemble a 4R linkage from the solutions to this design problem that could move its coupler smoothly through the task positions.

A fundamental problem in kinematic synthesis is the potential for a parallel assembly of chains, such as the 4R linkage constructed from two RR chains, to result in a workspace that separates the task positions either physically or with a linkage singularity. This is called *branching* [3], [4], known also as *mechanism defect* [5], [6]. One approach to avoiding the branching problem is to introduce free parameters by solving a reduced-design problem, which admits a manifold of solutions. Conditions that identify branching designs are imposed on this manifold to define subsets of useful designs [7]. Another approach is to use optimization theory to design the complete parallel system with branching conditions imposed as constraints on the solution [8], [9].

In this study, the authors introduced a new approach that presents both the design goal and evaluation of the resulting linkage. In this formulation, the authors solved the complete five multiply separated position synthesis problem, and allowed the designer to modify the design specifications, while evaluating features of the resulting design. Experiments showed that this procedure could yield an effective non-branching design to meets the designer's goals.

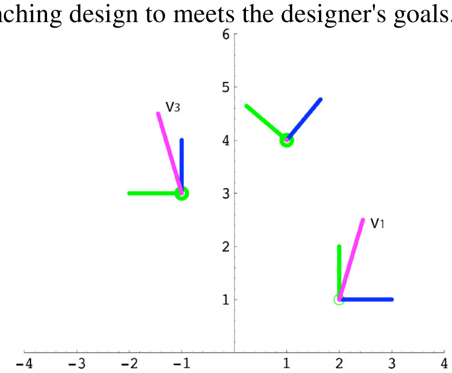

Figure 1. The five multiply separated position task, consisting of *i=3* specified positions $T_i = (\phi_i, p_{xi}, p_{yi})$ and *j=2* velocities $V_j = (\dot{\phi}_j, \dot{p}_{xj}, \dot{p}_{yj})$ defined in the first and third position

Synthesis Equations for an RR Chain

In order to synthesize a planar 4R chain, the authors formulated and solved the design equations for the planar RR serial chain. The analytical solution of these design equations yielded zero, two, or four sets of real values for the design parameters for RR chains that ensured that the floating link moved through the task positions. When two of these chains were connected in parallel, the workspace of the system was reduced from two to one dimension because the 4R chain had one degree-of-freedom. It happens that this one-dimensional workspace can take the form of a single closed curve with two singular configurations, or can be separated into two real curves, called *branches*, each of which may have two singular configurations. The focus here was on finding linkage designs that guide the floating link through all of the specified task positions such that they are on the same branch and do not encounter a singular configuration.

Kinematic Specification

The authors' formulation of the design equations for the RR chain followed those by Suh & Radcliffe [10] and Russel & Sodhi [11]. The kinematic specification consisted of three rotations and translations given by $T_i = (\phi_i, p_{xi}, p_{yi})$; $i=1,2,3$ and two sets of angular and linear velocities, defined in the first and third positions $V_j = (\dot{\phi}_j, \dot{p}_{xj}, \dot{p}_{yj})$; $j = 2,3$ where

$$(\dot{\phi}, \dot{p_{xj}}, \dot{p_{yj}}) = \frac{d}{dt}(\phi_i, p_{xi}, p_{yi}). \quad (1)$$

From Figure 1, $V_1 = (\dot{\phi}_1, \dot{p}_{x1}, \dot{p}_{y1})$ and $V_3 = (\dot{\phi}_3, \dot{p}_{x3}, \dot{p}_{y3})$ are the angular and linear task velocities defined in the first and third positions, respectively. The position data $T_i =$ (ϕ_i, p_{xi}, p_{yi}) is assembled into the 3 × 3 homogeneous transform equation (2),

$$[T_i] = \begin{bmatrix} \cos\phi_i & -\sin\phi_i & p_{xi} \\ \sin\phi_i & \cos\phi_i & p_{yi} \\ 0 & 0 & 1 \end{bmatrix}, \quad i = 1, 2, 3, \quad (2)$$

and the velocity data $V_j = (\omega_j, v_j, w_j)$ defines the 3 × 3 velocity matrix $[\Omega_i]=[\dot{T}_i][T_i^{-1}]$ given by

$$[\Omega_j] = \begin{bmatrix} 0 & -\dot{\phi}_j & \dot{p_{xj}} + \dot{\phi}_j p_{yj} \\ \dot{\phi}_j & 0 & \dot{p_{yj}} - \dot{\phi}_j p_{xj} \\ 0 & 0 & 0 \end{bmatrix}, \quad j = 1, 3. \quad (3)$$

Design Equations

The design parameters for the RR chain have the coordinates $\mathbf{G}=(G_x, G_y, 1)$ of the fixed pivot, the coordinates $\mathbf{W}^1 = (W_X, W_y, 1)$ of the moving pivot when the floating link is in the first position, and the length R of the link. Notice that in each task position the moving pivot $\mathbf{W}^i$ is constrained to lie at the distance R from **G**, so we have,

$$(\mathbf{W}^i - \mathbf{G}) \cdot (\mathbf{W}^i - \mathbf{G}) = R^2, \quad i = 1, 2, 3. \quad (4)$$

This equation also imposes a constraint on the velocity $\frac{d}{dt}\mathbf{W}^j$ of the moving pivot, such that in each task position

$$\frac{d}{dt}\mathbf{W}^j \cdot (\mathbf{W}^j - \mathbf{G}) = 0, \quad j = 1, 3. \quad (5)$$

The coordinates $\mathbf{W}^i$ of the moving pivot in each of the task positions are given by the formulas

$$\mathbf{W}^2 = [D_{12}]\mathbf{W}^1, \quad \text{and} \quad \mathbf{W}^3 = [D_{13}]\mathbf{W}^1, \quad (6)$$

where $[D_{1i}]=[T_i[T_1]^{-1}]$ is the relative displacement from the first task position to position i. Similarly, the velocities $\frac{d}{dt}\mathbf{W}^j$ are given by

$$\frac{d}{dt}\mathbf{W}^1 = [\Omega_1]\mathbf{W}^1, \quad \text{and} \quad \frac{d}{dt}\mathbf{W}^3 = [\Omega_3][D_{13}]\mathbf{W}^1. \quad (7)$$

The design equations (4) and (5) are quadratic in the design variables (G_x, G_y, W_x, W_y, R). However, these equations can be simplified to four bilinear equations in the four unknowns (G_x, G_y, W_x, W_y). McCarthy [14] demonstrates this for five position synthesis. Thus, there can be as many as four real solutions to this design problem.

Center Point and Circle Point Curves

The dimensions of a four-bar linkage with a specific number of positions of the coupler plane can be determined from the center-point and the circle-point curves. These curves could be obtained by plotting the cubic polynomials either in the fixed pivots (G_{xn}, G_{yn}), which results in center-point curves or in the moving pivots (W_{xn}, W_{yn}), which results in circle-point curves, where n is the number of solutions to the design problem. For the particular case of three positions and two specified velocities used in this study, the number of solutions is at most four and, therefore, four center-point curves and four circle-point curves were obtained (see Figures 2(a) and 2(b)).

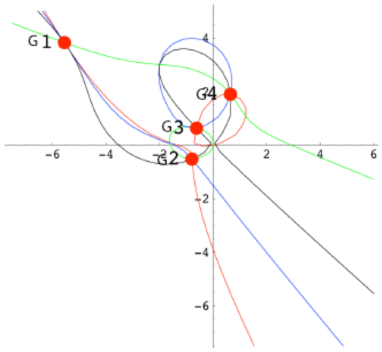

(a)

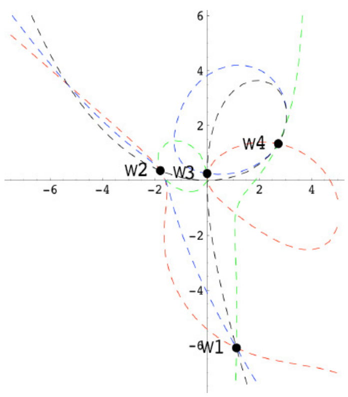

(b)

Figure 2(a) The points of intersection of the center-point curves define the coordinates of the four fixed pivots G. (b) The points of intersection of the circle-point curves define the coordinates of the four moving pivots W

Filemon's Construction and Waldron's Circle Diagram

As mentioned above, the dimensions of the theoretically possible 4R linkages, which pass through specific positions of the coupler plane, were determinable from the center-point and the circle-point curves. When using these curves for synthesis, some of the solutions did not perform the prescribed task due to constructional reasons [14]. The Filemon and Waldron constructions are helpful in defining the existence of a solution. In this paper, the authors show how to obtain a desired result in cases where there are no solutions, which satisfy the conditions.

Filemon's Construction

In the early seventies, Filemon [13] introduced a construction for the moving pivot of the input crank of a 4R linkage that ensures the smooth movement of the linkage through the task positions. The construction assumes that an output crank $G_{out}W^1_{out}$ has been selected. It is then possible to determine how this crank rotates to reach each of the design positions. Viewed from the coupler, this link sweeps out two wedge-shaped regions. Filemon showed that all that is necessary to guarantee that the resulting four-bar linkage will pass through the design positions was to choose the input moving pivot outside of these regions (see Figure 3). For any choice of the output moving pivot, W^1_{out} , a unique fixed pivot, G_{out}, can be determined. The positions that G_{out} can take relative to the moving frame are computed using the relative inverse displacements $[T^{-1}_{1i}]$ as:

$$G^i_{out} = [T^1_{1i}]G_{out}, \qquad (8)$$

where $[T^1_{1i}] = [T^{-1}_{1i}]$. The two angles, measured from G^1_{out} to G^2_{out} and G^2_{out} to G^3_{out} combine to form the wedge swept by the driven crank relative to the moving frame. The input moving pivot W^1_{in} should be chosen from outside of the wedge-shaped region. The resulting 4R linkage will pass through the design positions before the coupler lines up with the output crank, which defines the limit to the movement of the input crank.

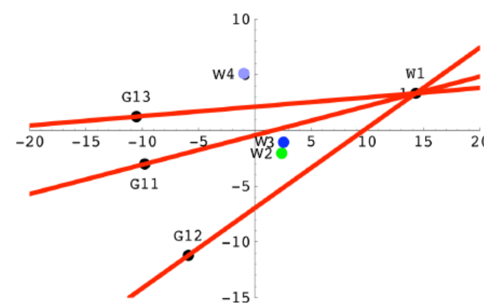

Figure 3. Filemon's Construction. *W1* is the chosen output moving pivot W^1_{out} W^1_{out} and G1 is it's corresponding unique fixed pivot G_{out}. The rotation of the output crank W1G1 identifies wedge-swept regions, defined by G11=G^1_{out}, G12=G^2_{out}, G13=G^3_{out} in this particular case, only *W4* can be chosen for an input moving pivot

The Pole Triangle

If there are three positions for a moving body, then the displacements can be considered in pairs and one can determine the poles P12, P23, P13 and the associated relative rotation angles $\phi_{12}, \phi_{23}, \phi_{13}$. It is easy to see that the displacements given by $T_{13} : (\phi_{13}, P13)$ is obtained by the sequence of the two displacements $T_{12}:(\phi_{12}, P12)$ followed by $T_{23}:(\phi_{23}, P23)$. Resulting in $\phi_{13}=\phi_{23}+\phi_{12}$. The three poles form a triangle, known as the pole triangle. Informatively, the image pole triangle is a mirror image of the pole triangle along a common side.

Waldron's Three-circle Diagram

In the mid seventies, Waldron [12] showed that if the output pivot W_{out}^1 rotates so that any of the angles measured from G_{out}^1 to G_{out}^2, or G_{out}^2 to G_{out}^3, or G_{out}^1 to G_{out}^3 is greater than or equal to π, there is no solution. This lead him to consider the point of viewing each side of the image pole triangle in $\frac{\pi}{2}$ and defining the three-circle diagram. The poles P12, IP23, P13 of the relative inverse displacements $[T_{12}^1],[T_{23}^1],[T_{13}^1]$ define an image pole triangle (see Figure 4). The center-point theorem applied to the image pole triangle yields the result that the moving pivot W_{out}^1 views the sides of this triangle at a rotation angle $-\alpha_{ik}/2$ of the coupler relative to the RR chain. Thus, for a point W and a side $p_{ij}^1 p_{jk}^1$ of the image pole triangle, we have the relation:

$$\cos\frac{\alpha_{ik}}{2}=\frac{(P_{ij}^1-W)\cdot(P_{jk}^1-W)}{|(P_{ij}^1-W)||(P_{jk}^1-W)|} \quad (9)$$

The points that have $-\alpha_{ik}/2=\frac{\pi}{2}$ lie on the circles:

$$\mathcal{C}_{ik}:\ (P_{ij}^1-W)\cdot(P_{jk}^1-W)=0. \quad (10)$$

The diameters of these circles are the segments $P_{ij}^1 P_{jk}^1$. The three circles, C_{12}, C_{23}, C_{13}, bound regions of points for which $-\alpha_{ik}/2>\frac{\pi}{2}$. Points outside of these circles, as well as points in regions where they overlap, can be used as moving pivots W_{out}^1. For these points, the output crank $G_{out}W_{out}^1$ has a solution. The result is a 4R linkage that moves through the three specified positions before it reaches a limit to the range of movement of the input crank.

In what follows, the authors showed that both the Filemon and Waldron constructions proved to be applicable in solving for non-branching solutions in the design of planar four-bar linkages. Waldron's diagram identified regions of moving pivots that ensured that Filemon's construction would yield useful driving pivots. It turns out that Filemon's construction gave non-branching solutions only when the input and/or output moving pivot(s) were chosen to be outside of the Waldron *bounded* region.

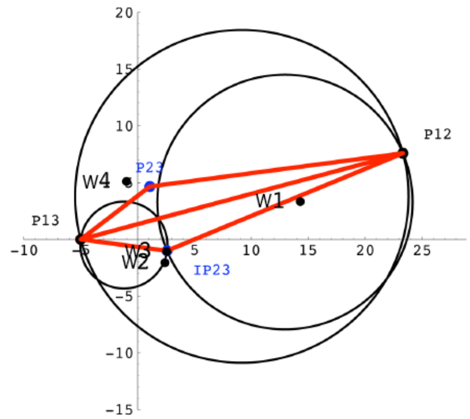

Figure 4. Waldron's Three-circle diagram. The poles P12, IP23, P13 define the image pole triangle and the poles P12, P13, P23 define the pole triangle. For this particular example only W1 and W2 can be considered as a moving pivots, since they lie at a places where two of the circles overlap

The Coupler Velocity Pole

A point of the moving plane that instantaneously has zero velocity may be located using equation (3), as follows:

$$[\dot{\mathrm{p}}_0]=\begin{bmatrix}0 & -\dot{\phi} & (\dot{p_x}+\dot{\phi}p_y)\\ \dot{\phi} & 0 & (\dot{p_y}-\dot{\phi}p_x)\\ 0 & 0 & 0\end{bmatrix}\begin{Bmatrix}p_{0x}\\ p_{0y}\\ 1\end{Bmatrix}=\begin{Bmatrix}0\\0\\0\end{Bmatrix}, \quad (11)$$

where **p** is an arbitrary point of the plane with specified motion. This leads to the equations for the coordinates of the velocity pole:

$$p_{0x}=p_x-\frac{\dot{p_y}}{\dot{\phi}},\ p_{0y}=p_y+\frac{\dot{p_x}}{\dot{\phi}} \quad (12)$$

Note that the location of the velocity pole for a plane motion mechanism can be defined in purely geometrical terms. The velocity pole or instant center for the coupler in a four-bar planar mechanism is located in the intersection of the line of centers of the two guiding cranks. Therefore, given the four solutions for the fixed **G** = (G_{ix}, G_{iy}) and for the moving **W**= (W_{ix}, W_{iy}) pivots of the 4R, we can express their relation to the coupler velocity pole in the two positions where task velocity specifications exist, can be expressed by:

$$\frac{p_{0y}-G_{iy}}{p_{0x}-G_{ix}}=\frac{W_{iy}-G_{iy}}{W_{ix}-G_{ix}},\quad i=1,2. \quad (13)$$

A property of the coupler velocity pole, defined in a particular position, is that it lies on the center-point curves. The image velocity pole, defined as p_{image}= (p_{oy} , - p_{ox}), lies on the circle-point curves. Therefore, modification of the task velocities in a particular position will result in alteration of the coupler velocity pole in this position, in reshaping the center-point and circle-point curves, and will result in shifting branching solution(s) in areas where the Waldron and Filemon constructions yield successful designs.

In the following sections, the authors apply equations (12) and (13) to one of the task positions with velocity specification in order to shift the branching solutions out of the bounded regions defined by Filemon's construction and Waldron's three-circle diagram.

Numerical Examples and Comments

The smooth motion of the coupler of a resulting design was evaluated using both Filemon's construction and Waldron's three-circle diagram. The Waldron diagram was used first since it identifies regions of moving pivots that ensure that Filemon's construction yields useful driving pivots. In other words, the solution existence was tested by the Waldron diagram, while Filemon's construction lead to the identification of the driving and the driven cranks. The main steps of this procedure are:

1) Plot Waldron's three-circle diagram, which depends only on task-position data. It is useful to plot also the task positions and velocities, as well as the coupler velocity poles (VP1 and VP3 in our case) in the positions, where task velocities are specified;

2) Chose two of the moving pivots, W_n, n=2, for the design of the planar four-bar and examine their position according to Waldron's construction. If one or both solutions need to be shifted outside of the bounded region to a "safe" location, proceed to the next step. If solution(s) do not need to be shifted, proceed directly to step 5;

3) Chose one of the two positions with velocity specification. Modify the coordinates of the velocity pole or the moving pivot, W_{xi} , W_{yi}, by applying equation (13). This will result in shifting W to a new "safe" location. Note, however, that changes in the W coordinates result in new coordinates for the corresponding fixed pivot G_{xi}, , G_{yi} ;

4) Solve equation(12) to obtain the new task velocity specifications, V $P_i = (\dot{p}_{oxi}, \dot{p}_{oyi})$, in the chosen position;

5) Plot the coupler velocity poles (VP1 and VP3 for this study) in the positions where task velocities are specified;

6) Use Filemon's construction and plot the four positions (G_{out} 1, G_{out} 2, G_{out} 3, G_{out} 4) the chosen unique pivot G_{out} can take. Plot also the solutions for the moving pivots (*W1, W2, W3, W4*) resulting from the synthesis of the 2R;

7) From the two chosen solutions, determine on input/driving and output/driven crank, using Filemon's construction. This will guarantee a successful four-bar linkage design; and,

8) Animate the four-bar linkage to ensure that it moves smoothly through the specified task.

In the end, it should be noted, that if the aim is towards a minimal deviation of the modified task from the originally specified one, then generating an array of uniform values in the vicinity of the originally specified velocity pole is needed. Next, the closest solution should be chosen and tested if it satisfies the Waldron and Filemon constructions.

Successful Design of a Four-bar Linkage: Example

The data set for this example is shown in Table 1.

Table 1. Data set

Position	Position $T = (\phi, p_x, p_y)$	Velocity $V = (\dot{\phi}, \dot{p_x}, \dot{p_y})$	Coupler Velocity Pole $VP = (p_{0x}, p_{0y})$
1	(0 deg, 3, 1)	(0.12 rad/s, 0.3, 1)	(-5.33, 3.5)
2	(45 deg, 1, 4)	not specified	not specified
3	(90 deg, -1, 3)	(-0.23 rad/s, 0, -0.23)	(-2, 3)

Figure 6(a) shows Waldron's construction, the coupler velocity poles in the first and third positions, VP1 and VP3, as well as the four solutions for W (smaller points) and G (thicker points), respectively. It can be seen that all fixed pivots, G_n , as well as the coupler velocity poles (VP1 and VP3) lie on the center-point curve (solid), while the moving pivots, W_n , are on the circle-point curve (dashed).

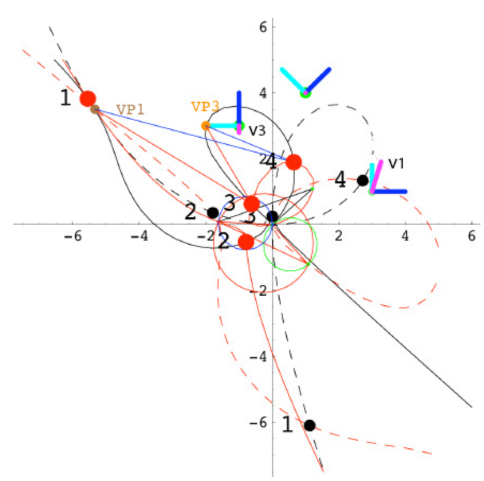

(a)

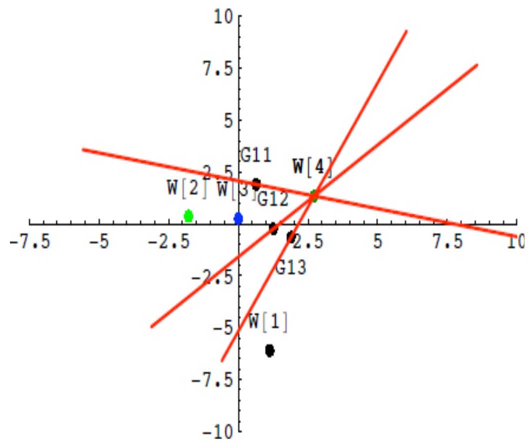

(b)

Figure 5. Solutions for case study I. (a) Waldron's circle diagram: the solutions W1, W2 and W4 (smaller points) can be used for driving pivots for the successful design of a four-bar linkage. (b) Filemon's construction: shows the chosen moving pivot W[4] and the arrangement of the rest moving pivots

It was assumed that there were no particular preferences of which two of the four solutions were choosen for the design of the four-bar linkage. The goal was to have a successful design that goes smoothly through the specified task. A quick examination of Waldron's diagram in Figure 5(a) shows that a non-branching solution can be obtained by using moving pivots **W**4 and **W**1. Both pivots are away from the Waldron bounded region. According to Filemon's construction (see Figure 5(b)), if **W**4 is chosen as the driving crank, **W**1 is outside of the Filemon wedged swept area and, therefore, can be used as a driven crank. The coordinates of the fixed and moving pivots of the chosen solutions are shown in Table 2.

Table 2. The fixed and moving pivots used to construct a fully operating four-bar linkage

Design	Fixed Pivot $G = (G_x, G_y)$	Moving Pivot $W = (W_x, W_y)$
Solution 4: Driving Crank	(0.65, 1.89)	(2.72, 1.34)
Solution 1: Driven Crank	(-5.54, 3.82)	(1.12, -6.09)

The smooth movement of the coupler of this successful design is shown in Figure 6.

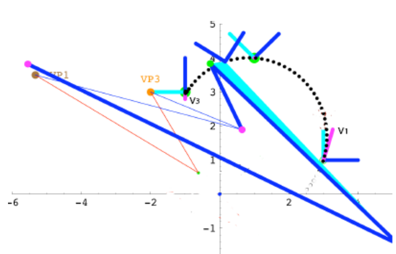

Figure 6. The four-bar linkage constructed from (G4, W4) and (G1, W1)

Case study I: *One of the solutions for the design of the four-bar linkage is in the bounded region.*

It was assumed that there was a need to assemble a four-bar linkage using the third and fourth [(W3, G3), (W4, G4)] real solutions of the synthesis equations for an RR chain. According to Waldron's three-circle diagram, the chosen moving pivot, W3, in Figure 5(a) would not work as a possible solution since it neither lies outside of the bounded area nor at a position where two of the circles overlap. The other chosen pivot, W4, was not a problem since it was out of the bounded area. The coordinates of the fixed and moving pivots of the chosen solutions are shown in Table 3.

Table 3. The fixed and moving pivots for case study one

Design	Fixed Pivot $G = (G_x, G_y)$	Moving Pivot $W = (W_x, W_y)$
Solution 4: Driving Crank	(0.65, 1.89)	(2.72, 1.34)
Solution 3: Driven Crank	(-0.62, 0.63)	(0.02, 0.25)

Figure 7 shows the movement associated with combining the third and fourth solutions, resulting in branching problems and, therefore, an unsuccessful four-bar linkage design. The first of the three specified task positions lies on the first branch and the second and third task positions are on the second branch. This example shows that the 4R chain cannot pass smoothly through the given task.

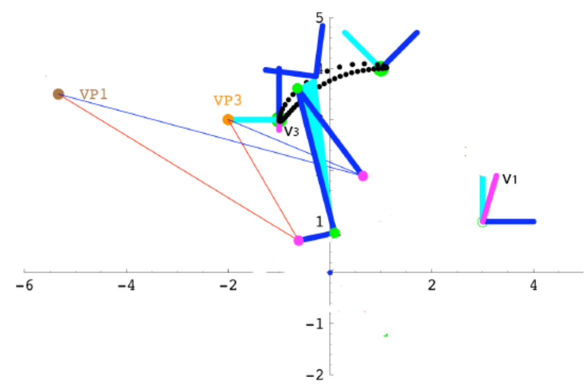

Figure 7. The four-bar linkage, constructed from (G3, W3) and (G4, W4) cannot pass through the specified task: a failed design

To solve the branching problem, equations (12) and (13) were applied. Pivot W3 was shifted to remain within Waldron's bounded circle but in an area where two of the circles overlap, i.e., from **W**3= (0.02, 0.25) (shown in Table 3) to **W**3= (0.61, 0.82) (see Table 5). Repositioning the **W**3 pivot at the new desired position resulted in modification of the coordinates of the fixed pivot, **G**3, as well as the coupler velocity pole, VP3, in the third position. The modified coupler velocity pole data in the third position, as well as the new data set for the linear velocity in the third position, are given in Table 4. The new coordinates of the moving pivot, **W**3, are shown in Table 5.

Table 4. The modified velocity set for case study one

Position	Coupler Velocity Pole $VP = (p_{0x}, p_{0y})$	New Velocity $V = (\dot{\phi}, \dot{p_x}, \dot{p_y})$
1	does not change	does not change
2	not specified	not specified
3	(2.81, 1.31)	(-0.23 rad/s, 0.39, 0.88)

Table 5. The modified coordinates for the moving pivot W3 and the fixed pivot G3 in the third position

Design	Fixed Pivot $G = (G_x, G_y)$	Moving Pivot $W = (W_x, W_y)$
Solution 4: Driving Crank	does not change	does not change
Solution 3: Driven Crank	(-0.64, 0.09)	(0.61, 0.82)

A fully operating 4R linkage is assembled in Figure 8, corresponding to the modified velocity. It can be seen that the chain is able to move smoothly through the given task and the path trajectory is tangent to the specified velocities.

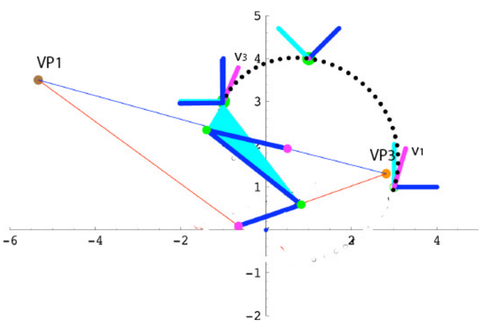

Figure 8. The modified four-bar linkage design for case study one

Case study II: *Driving/driven crank decision for the successful four-bar linkage design.*

Starting with the data set in Tables 1 and 3, the authors wanted to use the third and fourth solutions for constructing their four-bar linkage, similar to the first case study. Since the third solution yielded a branching problem, the authors chose to shift the moving pivot W3 outside of Waldron's bounded region, following the same procedure as in the first example. The modified velocity is given in Table 7.

Table 6. The modified coordinates of the moving pivot W3 and the fixed pivot G3 in the third position

Design	Fixed Pivot $G = (G_x, G_y)$	Moving Pivot $W = (W_x, W_y)$
Solution 3: Driving Crank	(-4.37, 2.21)	(2.11, -6.44)
Solution 4: Driven Crank	does not change	does not change

Waldron's diagram, the modified coupler velocity pole VP3, the new linear velocity in the third position, as well as the obtained coordinates for the moving pivot, W3, are given in Figure 9.

Table 7. The modified velocity set

Position	Coupler Velocity Pole $VP = (p_{0x}, p_{0y})$	New Velocity $V = (\dot{\phi}, \dot{p_x}, \dot{p_y})$
1	does not change	does not change
2	not specified	not specified
3	(-0.39, 2.17)	(-0.23 rad/s, 0.19, 0.14)

This time the authors chose to use solution three as a driving crank. In order to test the solution, they plotted Filemon's construction, shown in Figure 9(b), to determine which of the two cranks (**W**4, **G**4) or (**W**3, **G**3) should be chosen as the driving crank and which as the driven. The coordinates obtained for the input and output cranks are shown in Table 6, where the third solution was used as a driving crank.

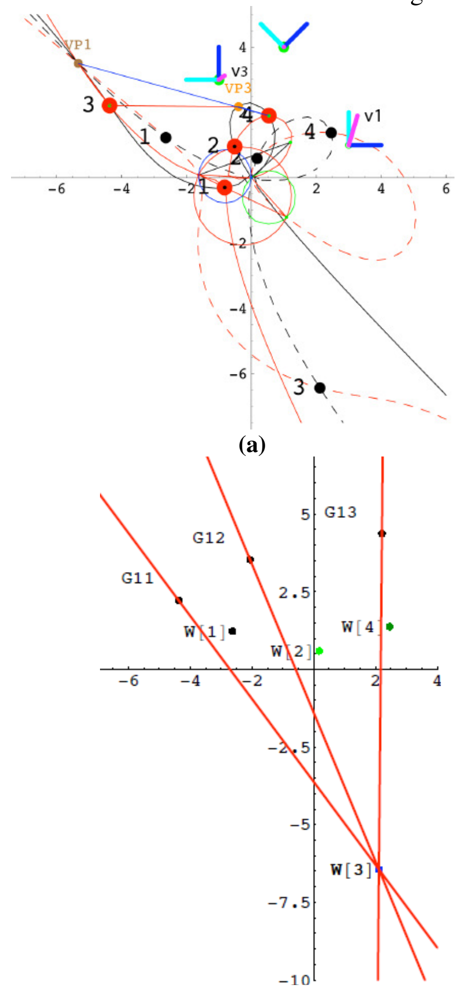

(b)

Figure 9. The modified solutions for case study II. (a) Waldron's three-circle diagram. (b) Filemon's construction for case-study II

Since **W**4 is outside of the wedge swept area, the coupling of these two solutions yields a fully operational design. The new working 4R linkage corresponding to the modified data set is assembled in Figure 10.

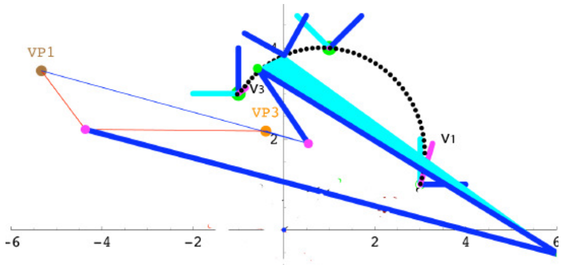

Figure 10. The successful four-bar linkage design for case study II

Summary

Specifying velocity constraints in certain task positions gives the designer control over the motion between the positions. The main contribution of the study was that both Filemon's construction and Waldron's three-circle diagram were found to have direct application in the planar four-bar linkage synthesis theory with task positions and velocity specifications. The task positions provide the geometric features of the position four-bar linkage synthesis, such as the pole triangle and Waldron's circle diagram. The study showed how to shift either chosen pivots or the velocity pole in one of the positions in order to reshape the coupler movement for non-branching solutions. The non-branching techniques discussed here can find direct application in the design of planar n-bar linkages, providing the designer the flexibility of modifying the task specifications as needed and, therefore, becoming a powerful tool for the future design of novel mechanical systems.

References

[1] D. Tesar and J. W. Sparks, "The Generalized Concept of Five Multiply Separated Positions in Coplanar Motion", *J. Mechanisms*, 1968, 3(1), 25-33.

[2] H. J, Dowler, J. Duffy, and D. Tesar, "A Generalised Study of Four and Five Multiply Separated Positions in Spherical Kinematics—II", *Mech. Mach. Theory*, 1978, 13:409-435.

[3] K. J. Waldron and E. N. Stevenson, Jr., "Elimination of branch, Grashof and Order Defects in Path-angle Generation and Function Generation Synthesis", *J. Mech. Design*, 1979, 101:428-437.

[4] K. C. Gupta, "Synthesis of Position, Path and Function Generating 4-Bar Mechanisms with Completely Rotatable Driving Links", *Mech. Mach. Theory,* 1980, 15, pp. 93-101.

[5] A. Bajpai and Kramer S., "Detection and Elimination of Mechanism Defects in the Selective Precision Synthesis of Planar Mechanisms", 1985, *Mech. Mach. Theory*, 20 (6), pp. 521-534.

[6] S. Balli and Chand S., "Defects in Link Mechanisms and Solution Rectification", *Mech. Mach. Theory*, 2002, 37, pp. 851-876.

[7] J. M. Prentis, "The Pole Triangle, Burmester Theory and Order and Branching Problems—II : The Branching Problem", *Mech. Mach. Theory,* 1991, 26(1): 31-39.

[8] A. Bajpai and S. Kramer, "Detection and Elimination of Mechanism Defects in the Selective Precision Synthesis of Planar Mechanisms", *Mech. Mach. Theory*, 1985, 20(6):521-534.

[9] M. DaLio, V. Cossalter, and R. Lot, "On the Use of Natural Coordinates in Optimal Synthesis of Mechanisms", 2000, *Mech. and Mach. Theory*, 35:1367-1389.

[10] Suh, C. H., and Radcliffe, C. W., Kinematics and Mechanisms Design, 1978, John Wiley and Sons, New York.

[11] Russell, K., and Sodhi R. S., "Kinematic Synthesis of Adjustable RSSR-SS Mechanisms for Multi-Phase Finite and Multiply Separated Positions", *Journal of Mechanical Design*, 2003, 125:847-853.

[12] K. J. Waldron, "Elimination of the Branch Problem in Graphical Burmester Mechanisms Synthesis for Four Finitely Separated Positions", *ASME Journal of Engineering for Industry*, 1976, 98B:176-182.

[13] E. Filemon, "Useful Ranges of Center-point Curves for Design of Crank-and-Rocker Linkages", *Mech. Mach. Theory*, 1972, 7: 47-53.

[14] McCarthy, J. M., Geometric Design of Linkages, 2000, Springer-Verlag, New York.

Biographies

NINA ROBSON is an assistant professor in Manufacturing and Mechanical Engineering Technology at Texas A&M University. Her research is in robotics, kinematics of motion, and biomechanics. Her e-mail address is ninarobson@tamu.edu.

MICHAEL MCCARTHY is a professor in Mechanical Engineering at University of California, Irvine. His research is in design of mechanical systems, computer aided design, and kinematic theory of spatial motion. He can be reached at jmmccart@uci.edu.